Electric Heater Development and Performance Data for a Mach 14 Wind Tunnel

J. F. Reed,* C. W. Peterson,† and W. H. Curry‡
Sandia Laboratories, Albuquerque, N. Mex.

A high-pressure Mach 14 testing capability has been added to the Sandia Laboratories Hypersonic Wind Tunnel (HWT) facility. Of particular significance is the new electric heater which was developed for this addition. The heater is considered unique. Its heating elements are groups of rectangular screens oriented normal to the flow and positioned at several longitudinal stations. The heater is extremely compact in size and operates directly from three-phase alternating current. It can deliver up to 1 Mw of power to the test gas at pressures as high as 2000 N/cm^2 (2900 psia) for a 60 sec run. Stagnation temperatures to 1400 K (2500°R) are achieved. Pressure and temperature calibrations show that the flow in the 46 cm (18 in.) diameter test section is satisfactory for research and development experimentation.

Nomenclature

d_c	= diameter of control orifice, cm (in.)
d_n	= diameter of nozzle throat, cm (in.)
e_1, e_2, e_3, I^*, J^*, K^*, K_T, J_T	= real gas parameters defined by Randall in Ref. 1
M	= Mach number
P_c	= stagnation pressure in the control orifice, N/cm^2 (psi)
P_o	= stagnation pressure at the electric heater, N/cm^2 (psi)
P_t	= pitot pressure, N/cm^2 (psi)
P_w	= wall static pressure, N/cm^2 (psi)
P_∞	= freestream static pressure, N/cm^2 (psi)
T_c	= stagnation temlture at the control orifice, K (°R)
T_o	= stagnation temperature in the electric heater, calculated from Eq. (1), K (°R)
T_{t_l}	= local total temperature in the boundary layer, K (°R)
U	= velocity, m/sec (fps)
Y	= transverse distance across tunnel, cm (in.)
Z	= axial distance downstream of nozzle throat, cm (in.)
$\beta_{c,n}$	= real gas mass flow parameter in control orifice (β_c) and nozzle throat (β_n)
γ	= perfect gas ratio of specific heats
o	= density, kg/m^3 (slugs/ft^3)

Subscripts

e	= condition at the edge of the wall boundary layer
2	= conditions behind a normal shock

Presented as Paper 74-616 AIAA 8th Aerodynamics Testing Conference, Bethesda, Md., July 8-10, 1974; submitted Aug. 1, 1974; revision received November 20, 1974. This work was supported by the U.S. Energy Research and Development Administration. The authors wish to express deep appreciation for the contributions of D. C. Nichols, FluiDyne Engineering Corporation, Project Engineer on the design of the heater; and of C. C. Tolbert and D. R. MacKenzie, Sandia Laboratories, for their assistance in the heater installation and shakedown.

Index category: Research Facilities and Instrumentation.

*Member of Technical Staff, Experimental Aerodynamics Divison. Associate Fellow AIAA.

†Supervisor, Experimental Aerodynamics Division. Member AIAA.

‡Member of Technical Staff, Aeroballistics Division. Associate Fellow AIAA.

Introduction

SANDIA Laboratories' Hypersonic Wind Tunnel[2] (HWT) was placed in operation in 1962. The original facility is shown schematically in Fig. 1. Separate nozzles provide nominal Mach numbers of 5, 7, and 11; each nozzle has a test section which is 46 cm (18 in.) in diameter. All components were designed for a maximum stagnation pressure of 200 N × cm^2 (300 psi)

In recent years, the need arose for higher Mach and Reynolds numbers, thus necessitating a much higher stagnation pressure capability. Also, certain undesirable operational features, such as contamination of the flow by dust from the alumina pebbles in the heater and frequent difficulties with the quick opening hot valve, indicated that the heating system should be replaced with an electric type. A major modification program was implemented, and the first step was to provide a high-pressure $M = 14$ capability utilizing an electric screen heater.

Certain operational and physical constraints made the development of an electric heater for the $M = 14$ facility particularly difficult. A major constraint was that lower Mach number nozzles be operated using the pebble bed heater without interruption during the implementation of the $M = 14$ capability. All nozzles are mounted on a revolver located between the quick opening valve and diffuser inlet. Since there was no room for the electric heater in front of the revolver with the pebble bed heater in place, the electric heater had to be located on the revolver in line with the $M = 14$ nozzle for most efficient operation. Consequently, the heater had to be compact, yet capable of delivering up to 1 Mw of power to the test gas at pressures as high as 2000 N/cm^2 (2900 psia) for 60 sec per run.

The electric heater which was developed is considered unique. The heating elements are groups of rectangular screens oriented normal to the flow and positioned at several longitudinal stations. The heater operates directly from three-phase alternating current. To the authors' knowledge, there is no similar heater in existence. The purpose of this paper is to present the details of the heater design, to describe the $M = 14$ configuration, and to discuss the performance of the facility as measured by flow surveys in the test section inviscid core and boundary layer.

$M = 14$ Electric Heater and Associated Components

The new $M = 14$ facility is shown schematically in Fig. 2. It consists of nitrogen supply, heater, and nozzle as subsequently described.

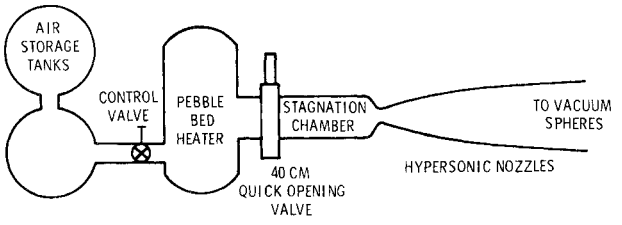

Fig. 1 Original HWT facility.

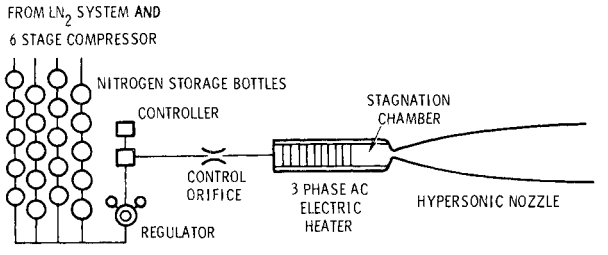

Fig. 2 New $M=14$ facility.

Nitrogen Supply and Control Components

Nitrogen is supplied from a 5.68 m^3 (1500 gal) liquid nitrogen reservoir. The nitrogen is gasified and fed at a controlled pressure of 21 N/cm^2 (30 psia) to the second stage of a six-stage, 2.38m^3/min (84 scfm) air-cooled compressor. The compressed nitrogen is stored at 6900 N/cm^2 (10,000 psia) in 20 bottles totaling 1.4 m^3 (50 cubic ft). At typical $M=14$ operating conditions, pumping capacity is sufficient for a 65 sec run every hour.

Immediately downstream of the high-pressure storage bottle farm is a regulator which reduces the pressure in the line to 3450 N/cm^2 (5000 psi). A pressure controller is used to set the stagnation pressure at the control orifice (P_c), and a thermocouple records the stagnation temperature at the control orifice (T_c). The flow through the orifice is always sonic, ensuring that the mass flow rate into the electric heater does not change when heater power is suddenly applied. The control orifice also makes it possible to regulate P_c so that the desired value of the heater stagnation pressure (P_o) and temperature (T_o) shall be obtained after the heater is turned on. An expression relating P_c to P_o, T_c, and T_o was derived assuming a one-dimensional steady-state mass flux balance between the flow entering the control orifice and the flow leaving the nozzle throat. The governing equation, which is valid for any gas which may be described by a Beattie-Bridgeman equation of state with variable specific heats, is:

$$\left(\frac{P_c}{P_o}\right)^2=\left(\frac{T_c}{T_o}\right)\left(\frac{d_n}{d_c}\right)^4\left(\frac{\beta_n}{\beta_c}\right)^2$$

where

$$\beta=\left[(I^*)^{1/2}\left(\frac{J_T}{J^*+[(\gamma-1)/2]I^*}\right)^3-\frac{K^*}{K_\Gamma}\right]\div[1+e_1\rho+e_2\rho^2+e_3\rho^3]$$

(Starred quantities indicate that these parameters are evaluated at local sonic conditions.)

Electrical Supply and Control Components

Power to energize the heater is provided from a 44 kV/4.16 kV, 10 Mw substation. Power control is provided by a General Electric 5-Mw Inductrol Controller. The Inductrol output voltage is continuously variable from 0.66 to 1.33 times the input voltage. Thirty seconds are required to traverse the entire range from 2773 to 5546 volts. The Inductrol output is fed through a drawout air-break contactor, which serves as heater start-stop switch, to a 5433/70 volt, delta-connected, 1000 KVA power transformer. Bus bars and water-cooled cables provide the feed from the secondary of this transformer to the $M=14$ electric heater. Voltage control is provided from the tunnel operator's console. In normal operation, the starting voltage and running voltage are preset prior to the run and actuated by microswitches after tunnel flow is started.

Electric Nitrogen Heater§

The electric nitrogen heater is unique in several ways. Constraints on its size have resulted in a very compact unit; it is 34.3 cm (13.5 in.) in diameter, 87.6 cm (34.5 in.) long and weighs about 405 kg (890 lb). Its small size permits it to be mounted on the HWT revolving nozzle rack and greatly simplifies storage and handling. It is the only wind tunnel electric heater, to the authors' knowledge, which utilizes in-line screens and three-phase alternating current power.¶ The use of ac power did not make the heater design less difficult, but it greatly reduced the cost of power supply and control equipment.

A photograph of the heater internals is shown as Fig. 3, and an electrical schematic of the heater is shown in Fig. 4. The three-phase power transformer provides approximately 70 volts and 8500 amps to each phase at nominal $M=14$ operating conditions. Heating of the nitrogen gas takes place in a channel which is 7.6 cm (3 in.) square and 66 cm (26 in.) long. The side walls are made of electrically insulating, low expansion titanium silicate glass. As the nitrogen flows along the channel, it passes through heated screens which are fastened to the bus bars at the top and bottom. Screens are located at 14 stations in the passageway. The first screen station contains one fine-mesh nichrome screen, which smooths out the flow nonuniformities entering the heating channel, and three porous inconel screens. Each of the five screens at the next three stations are porous mesh inconel. These first four screen stations are connected in series to one phase of the three phase delta power supply. The second phase consists of five stations of porous tungsten screens with four screens per station, and the third phase consists of five stations with five tungsten screens at each station.

The specific combination of screens per station, screen material, and stations per phase discussed above gives nearly balanced loading of each phase in the ac power supply at the nominal $M=14$ operating conditions. Porous screens are required to prevent large pressure losses along the channel; when too many fine-mesh screens are used, the increase in pressure in the channel forces the nitrogen gas to flow around the edge of the heater screens, causing them to overheat and break. Nonuniform heating at any screen station is another cause of screen failure. In order to avoid this problem, "half-screen" sections, with screen material only at the edges of the channel, are used in the second and third stations of the first phase to add extra heat near the side walls to compensate for conduction heat losses. Nickel deflector plates are mounted on the side walls between each screen station to mix the gas

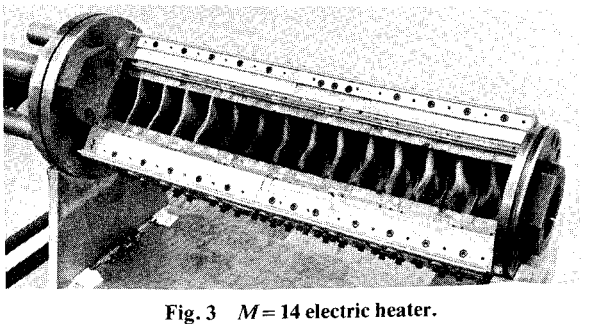

Fig. 3 $M=14$ electric heater.

§Detailed design and construction of the electric heater was done by FluiDyne Engineering Corporation under contract to Sandia Laboratories.

¶A heater using an annular screen and dc power is described by Clark and Ellison[3]

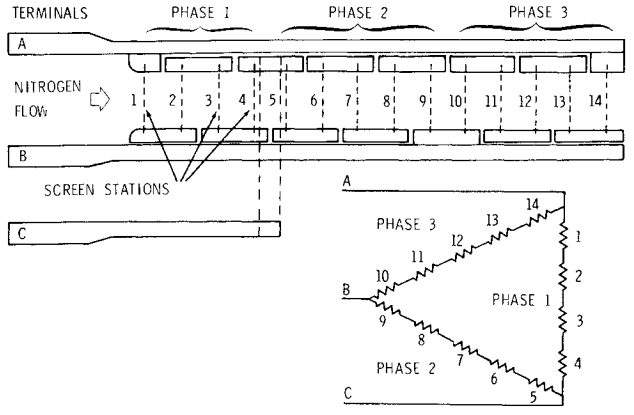

Fig. 4 Electrical schematic of $M = 14$ heater.

Table 1 Specifications of heater screens

Heater station	Screen number	Screen material	Screen weave (wires/in.)	Wire diameter (inches)		Remarks
1	1	Nichrome V	450×20	0.0045	Vert.	
			Dutch Twill	0.010	Horiz.	
1	2-4	Inconel 600	40×40	0.010	Vert.	
			Square Mesh	0.010	Horiz.	
2-3	1	Inconel 600	40×40	0.010	Vert.	Screens with center half cut out
			Square Mesh	0.010	Horiz.	
2-3	2-5	Inconel 600	40×40	0.010	Vert.	
			Sq Mesh	0.010	Horiz.	
4	1-5	Inconel 600	40×40	0.010	Vert.	
			Square Mesh	0.010	Vert.	
5-9	1-4	Tungsten	30×25	0.010	Vert.	
			Twill	0.010	Horiz.	
10-14	1-5	Tungsten	30×25	0.010	Vert.	
			Twill	0.010	Horiz.	

and to prevent hot spots from forming. Technical data on the various screens is presented in Table 1.

When the power is applied to the heater during startup, the temperature of the screens and the energy input to the test gas vary with time and heater screen location. The resulting transient behavior of the gas in the heater has been approximated numerically by dividing the heater into four chambers and assuming no spacial variations in gas properties within each chamber. At each time interval during startup, the temperature, pressure, and total mass in the chambers are computed by equating the electrical energy input to the increase in gas temperature minus the net convection of energy out of each chamber. Figure 4 shows the computed time-variation of mass flow rate at three locations in the heater channel. In order to avoid burning out the heater screens during startup, the heater is turned on at 80% of the power required to attain the desired operating conditions. Once the transients in mass flow

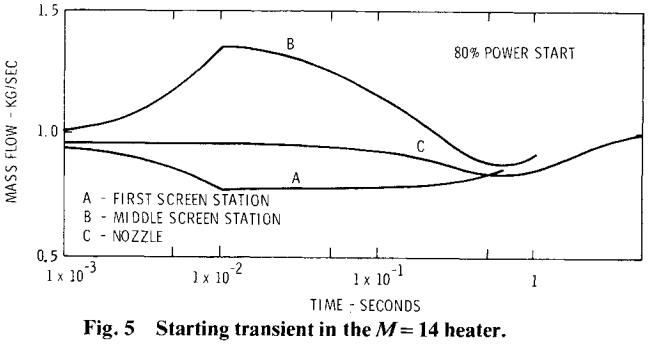

Fig. 5 Starting transient in the $M = 14$ heater.

rate have passed, the Inductrol is used to increase the power to its full value. This starting process requires 20 sec, but the remaining 45 sec of run time is adequate for obtaining data.

The original heater design called for platinum heater screens so that air could be used as the test gas, but, after repeated failures of the platinum screens, tungsten screens and nitrogen gas were substituted. With this new screen material, the heater performs satisfactorily as long as the nitrogen gas is sufficiently pure. However, very small amounts of oxygen in the test gas will destroy the screens immediately. To preserve the tungsten screens during several months of use, the $M = 14$ heater is operated only if the nitrogen contains fewer than 6 ppm of oxygen. The nominal oxygen content of the nitrogen test gas during testing to date has been below 3 ppm.

Text experience has proven the heater to be long-lived, with more than 300 runs being made in one case between screen burnouts. Screen replacement is quite simple, requiring about 2 hours, since usually only one or two of the 14 screen stations sustain damage during a burnout. No danger is involved; a burnout merely results in a loss of stagnation temperature and pressure. The complicated arrangement of number of screens per station, screen material, and screen porosity was developed over some two years of testing and redesign, and has been proven to be necessary to reduce the screen failure to the present low value.

Test experience has proven the heater to be long-lived, with more than 30 runs being made in one case between screen burnouts. Screen replacement is quite simple, requiring about 2 hours, since usually only one or two of the 14 screen stations sustain damage during a burnout; no danger is involved, a burnout merely results in a loss of stagnation temperature and pressure. The complicated arrangement of number of screens per station, screen material and screen porosity was developed over some two years of testing and redesign, and has been proven to be necessary to reduce the screen failure rate to the present low value.

The heater has been operated at stagnation pressures to 2000 N/cm^2 (2900 psia) and stagnation temperatures in excess of 1400 K (2500°R).

$M = 14$ Nozzle

The $M = 14$ nozzle consists of a water-cooled throat section, two uncooled expansion sections, and a 46 cm (18 in.) diam test section whose contour is a continuation of the nozzle wall shape. The throat section is zirconium copper; the two expansion sections and the test section are made of an aluminum and magnesium alloy. Instrumentation ports are located in the walls of these sections at ten stations along the axis, and five additional ports are positioned around the nozzle near the test section to examine the symmetry of the flow. The test section has four window ports which can be filled with window plugs contoured to the test section wall shape if visual coverage of the test is not required. One of these contoured plugs also has instrumentation ports at three axial stations.

Safety Considerations

Any facility such as the HWT possesses numerous potential safety hazards. The combination of potential energy in the high pressure stored gas and kinetic energy in the electric heater made safety considerations of prime importance throughout the design of the $M = 14$ addition. Every effort was taken to make the operation as foolproof as possible. Each isolated portion of the compressed gas system is equipped with a safety valve of the appropriate rating. The tunnel operator must follow a precisely prescribed procedure during the tunnel startup and operation. Sequential safety switches prevent any step in the operation from being taken unless all previous steps are complete.

In many ways, the electric heater itself has inherently safe characteristics. The small mass of gas in the heater repre-

sents little potential energy. No circuit breakers or fuses are necessary in the power circuit; the heater itself acts as an excellent quick-blow fuse. The small amount of gas trapped between the control valve and the nozzle would permit quick shut-down should the nozzle fail.

Performance of the $M = 14$ Wind Tunnel

In the sections which follow, tunnel operational limitations, inviscid core pitot pressure rake surveys, nozzle wall temperature and pressure measurements, and nozzle boundary-layer profiles will be presented to indicate the overall performance of the electrically heated $M = 14$ facility.

Operating Range

The range of operating stagnation pressures and temperatures is shown in Fig. 6. The maximum operational temperature limit of 1400 K (2500°R) was established to avoid damaging the nozzle throat and internal components of the electric heater. The minimum pressure boundary was determined experimentally by requiring at least 50 sec of run time before observing tunnel stall. The maximum allowable pressure limit of 2000 N/cm^2 (2900 psia) is determined by heat transfer and thermal stress considerations in the nozzle throat.

The minimum stagnation temperature boundary of the $M = 14$ operating range is determined by the onset of condensation in the test section. Although a semi-empirical method for predicting the onset of condensation has been reported by Daum and Gyarmathy,[4] this technique is conservative and may not account for all of the parameters affecting condensation which are unique to each facility (e.g., the amount of moisture in the test gas). Consequently, an experimental investigation of condensation in the $M = 14$ nozzle was conducted using wall static pressures and a pitot probe on the centerline of the test section. Stagnation pressures and temperatures were gradually reduced from values above the condensation line while pitot and static pressures were monitored. The onset of condensation was taken to be the temperature at which the ratio P_w/P_o or P_t/P_o departed from a nearly constant value.** The results of these experiments are consistent with data from other nitrogen tunnels, as shown in Fig. 7. Since accurate measurements of condensation onset are difficult to make due to hysteresis effects in the condensation phenomenon, testing in the $M = 14$ nozzle is conducted at stagnation temperatures which are at least 60 K higher than the minimum temperature line given in Fig. 6.

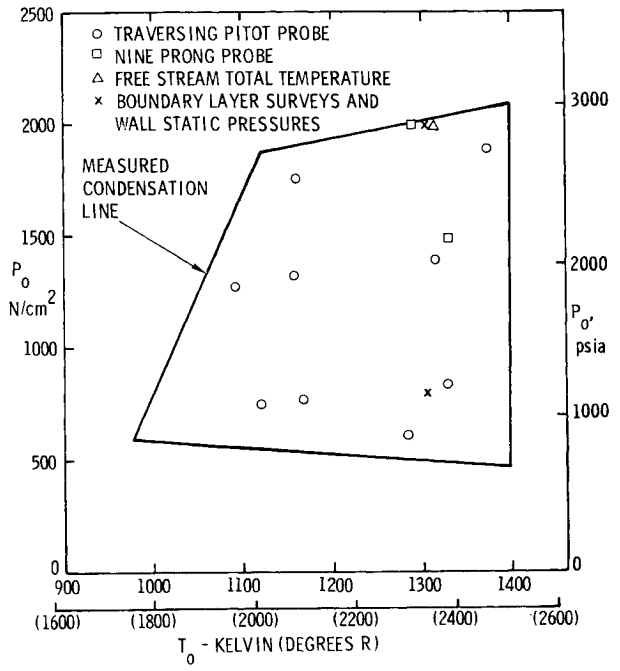

Fig. 6 Operating range of the $M = 14$ facility.

**These ratios vary slightly in the absence of condensation due to changes in the nozzle wall boundary layer displacement thickness.

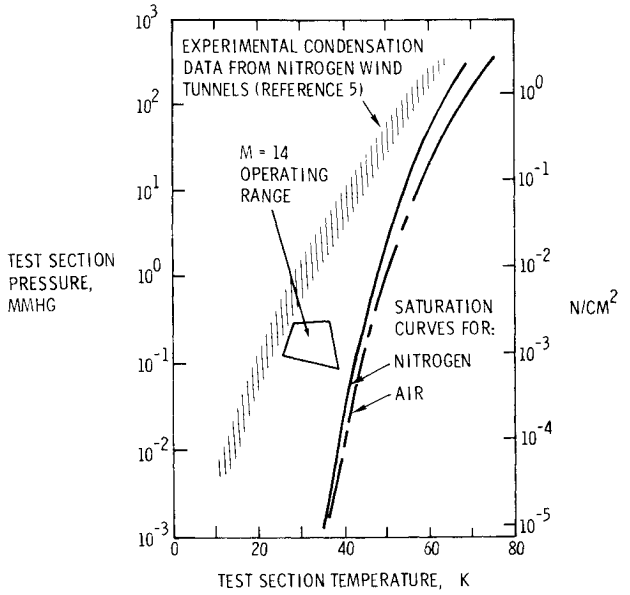

Fig. 7 Onset of condensation in the $M = 14$ nozzle.

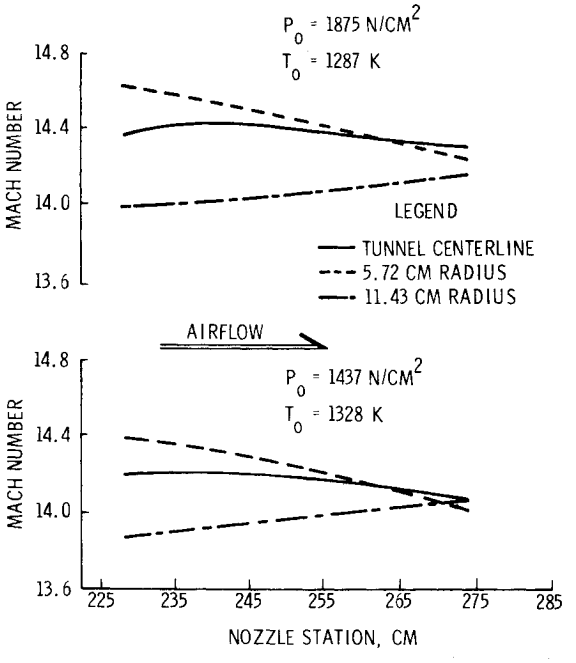

Fig. 8 Axial Mach number distribution in the $M = 14$ nozzle.

Inviscid Core Surveys

The preliminary calibration presented in Fig. 8 was obtained by mounting a nine-prong pitot rake at four stations along a 45.7 cm (18 in.) test section length. The rake has probes at transverse stations 5.72 and 11.43 cm (2.25 and 4.50 in.) horizontally and vertically from the tunnel centerline. The calibration was conducted at two tunnel conditions: $P_o = 1437$ N/cm^2 (2084 psia) at $T_o = 1328$ K (2390°R) and $P_o =$ N/cm^2 (2720 psia) at $T_o = 1287$ K (2316°R). The Mach number data in Fig. 8 (and all subsequent freestream Mach number data) were calculated from pitot pressure measurements and stagnation pressure assuming the Beattie-Bridgeman equation of state with variable specific heats. The centerline Mach

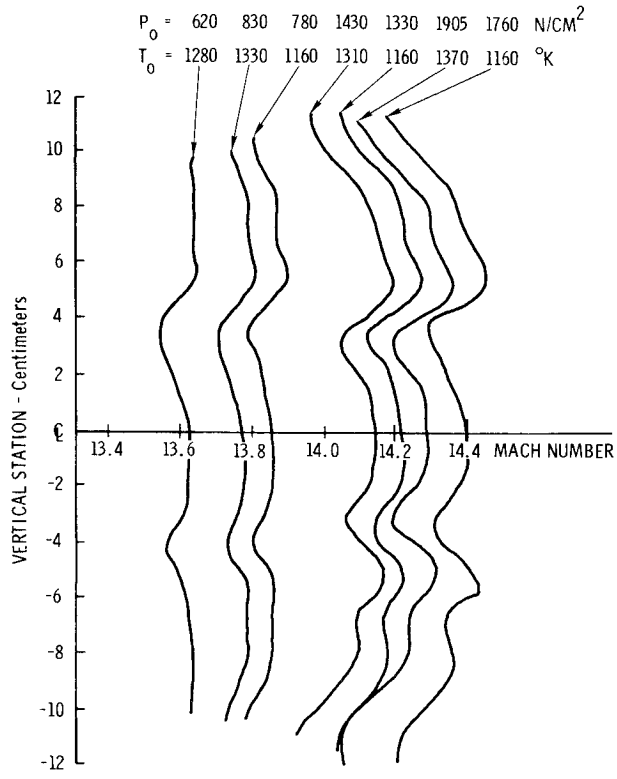

Fig. 9 Vertical Mach number distribution in the $M = 14$ nozzle.

number gradients were quite good at both test conditions, being less than ±0.6% from the mean. The flow at radial stations 5.72 cm (2.25 in.) showed a decreasing Mach gradient of -0.008 per cm at the inner radial stations and an increasing Mach gradient of +0.0045 per cm at the outer stations.

A three-prong traversing pitot probe rake was installed in the tunnel at a station 253.5 cm (99.7 in.) from the nozzle throat to obtain a map of the inviscid core flow in the vertical plane. Runs were made at the conditions shown in Fig. 9, and data points were taken at intervals of about 0.25 cm (0.1 in.). Although the survey extended well into the nozzle wall boundary layer, only the inviscid core data are presented in this figure. As can be seen, the vertical Mach number variation at the probe station, which is near the center of rotation of the HWT pitching sector—station 250.3 cm (98.5 in.)—is less than ±0.17 over a 20 cm (8 in.) diam core at all test conditions.

Since a thorough understanding of heat transfer rates on hypersonic vehicles is essential in most developmental programs, the $M = 14$ nozzle must generate uniform stagnation temperatures across the freestream inviscid core so that accurate heat transfer data may be obtained in the facility. Because the velocity in the heater is low, it was suspected that buoyancy effects may cause considerable temperature stratification in the flow upstream of the nozzle throat. Measurements of total temperature in the vertical plane of the heater exit and the test section not only confirmed the presence of buoyancy effects at the heater exit, but also showed that temperature stratification was not eliminated during the expansion through the nozzle throat. Several devices have been built to mix the gas before it passes through the nozzle throat. Total temperature surveys across the test section inviscid core showed that even a simple contraction disk is effective in reducing total temperature gradients in the test section.

Nozzle Wall Measurements and Boundary-Layer Surveys

Nozzle wall static pressure, nozzle wall temperature and boundary layer pitot pressure, total temperature, and cone-static pressure surveys were made at several stations along the

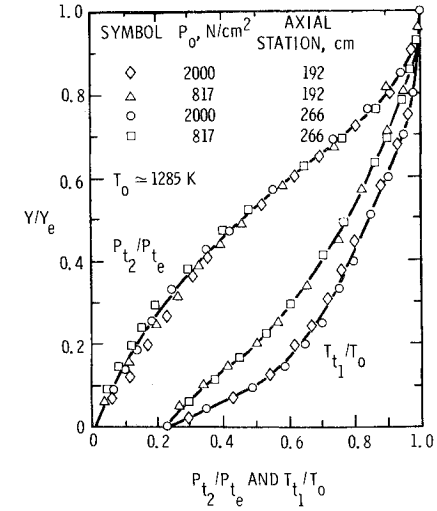

Fig. 10 $M = 14$ boundary-layer pitot and total temperature measurements.

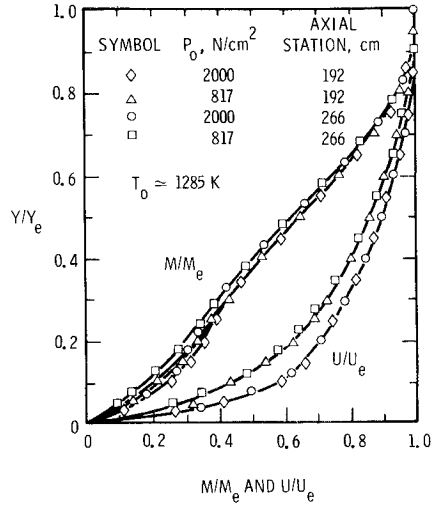

Fig. 11 $M = 14$ boundary-layer Mach number and velocity profiles.

nozzle. These data were obtained to check the validity of the turbulent boundary-layer assumptions which were used to correct the $M = 14$ nozzle contour for viscous effects. Reference 5 contains a detailed description of these boundary-layer measurements, but the most important results are summarized in this section.

Nozzle wall static pressure results indicate that the nozzle wall boundary layer is not separated at either the low or high freestream Reynolds number operating conditions. These pressure data, coupled with estimates of wall pressures in the cooled portion of the nozzle, were used in conjunction with an analysis by Back et al.,[6] to show that relaminarization of the turbulent boundary layer is improbable at either test condition. The insensitivity of boundary-layer pitot profiles to Reynolds number (Fig. 10) is further evidence that these nozzle wall boundary layers are turbulent from the throat to the test section.

The results of the turbulent boundary-layer surveys demonstrate the inadequacies in common turbulent boundary-layer prediction techniques used in the calculation of hypersonic nozzle contours. Nearly every nozzle wall boundary-layer analysis (examples are given in Refs. 7-10) contains approximations for the shape of the velocity profile, the skin friction, and the dependence of velocity upon temperature. Each approximation assumes that these relationships are functions of the local wall properties and boundary-layer edge conditions. However, the present measurements indicate that

total temperature profiles (Fig. 10) and velocity profiles (Fig. 11) are more dependent upon upstream wall temperature history than upon local wall temperature. The effects of upstream pressure history have been observed in other nozzle wall boundary layers. Furthermore, cone-static pressure measurements indicate that significant pressure gradients exist across the nozzle wall boundary layer, contrary to the assumptions implicit in the integral equations which govern the prediction techniques. These results suggest that transformation solutions to the compressible turbulent boundary-layer problem are inherently unable to model the basic flow phenomena correctly. Finite-difference numerical techniques have the advantage of using equations of motion which contain information on the upstream history of the flow, but even these techniques must be modified to include the effects of static pressure variations across the boundary layer.

Conclusions

A compact 1 Mw electric heater was developed to provide the Hypersonic Wind Tunnel with a high-pressure Mach 14 testing capability. It is capable of heating the test gas to temperatures as high as 1400 K (2500°R) at 2000 N/cm^2 (2900 psia). After extensive development and testing, the heater has proven to be both reliable and efficient. Typically, two hundred 60-sec runs can be made before heating elements must be replaced. Pressure and temperature calibrations in the $M = 14$ nozzle which uses this heater show that the flow quality is adequate for conducting experimental research and development programs in aerodynamics and fluid mechanics.

References

[1] Randall, R. E., "Thermodynamic Properties of Gases: Equations Derived from the Beattie-Bridgeman Equation of State Assuming Variable Specific Heats," AEDC-TR-57-10, Aug. 1957, Arnold Engineering Development Center, Tullahoma, Tenn.

[2] Maydew, R. C., "Sandia Laboratory Aerodynamic Test Facilities," SC-4937(M), Sept., 1963, Sandia Laboratories, Albuquerque, N.M.

[3] Clark, F. L., and Ellison, J. C., "Recent Work in Flow Evaluation and Techniques of Operations for the Langley Hypersonic Nitrogen Facility," presented at the Fifth Hypervelocity Techniques Symposium, Denver, Colo., March 1967.

[4] F. L., and Gyarmathy, G., "Condensation of Air and Nitrogen in Hypersonic Wind Tunnels," *AIAA Journal*, Vol. 6, March 1968, pp. 458-465.

[5] Peterson, C. W., "Pressure and Temperature Measurements in a Cold-Wall Hypersonic Turbulent Boundary Layer," presented at the 12th Heat Transfer and Fluid Mechanics Institute, Oregon State University, Corvallis, Ore., June 1974.

[6] Back, L. H., Cuffel, R. F., and Massier, P. F., "Laminarization of a Turbulent Boundary Layer in Nozzle Flow," *AIAA Journal*, Vol. 7, April 1969, pp. 730-733.

[7] Glowacki, W. J., "Fortran IV (IBM 7090) Program for the Design of Contoured Axisymmetric Nozzles for High Tempeture Air," NOLTR 64-219, Feb. 1965, Naval Ordnance Lab., White Oak, Md.

[8] Edenfield, E. E., "Contoured Nozzle DON AND Evaluation for Hotshot Wind Tunnels," AIAA Paper 68-369, San Francisco, Calif., 1968.

[9] Sivells, J. C., "Aerodynamic Design of Axisymmetric Hypersonic Wind Tunnel Nozzles," *Journal of Spacecraft and Rockets*, Vol. 7, Nov. 1970, pp. 1292-1299.

[10] Tetervin, N., "NOL Hypervelocity Wind Tunnel Report No. 3: Theoretical Analysis of the Boundary Layer in the Nozzle," NOLTR 71-7, Feb. 1971, Naval Ordnance Lab., White Oak, Md.